NASA TECHNICAL NOTE

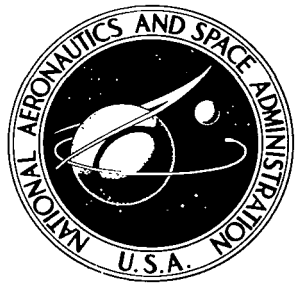

NASA TN D-6287

NASA TN D-6287

AMPLIFICATION BY WAVE DISTORTION OF THE DYNAMIC RESPONSE OF VAPORIZATION LIMITED COMBUSTION

by Marcus F. Heidmann

Lewis Research Center
Cleveland, Ohio 44135

NATIONAL AERONAUTICS AND SPACE ADMINISTRATION • WASHINGTON, D. C. • MAY 1971

1. Report No.	2. Government Accession No.	3. Recipient's Catalog No.
NASA TN D-6287		

4. Title and Subtitle
AMPLIFICATION BY WAVE DISTORTION OF THE DYNAMIC RESPONSE OF VAPORIZATION LIMITED COMBUSTION

5. Report Date: May '1971
6. Performing Organization Code:

7. Author(s)
Marcus F. Heidmann

8. Performing Organization Report No.: E-6049

9. Performing Organization Name and Address
Lewis Research Center
National Aeronautics and Space Administration
Cleveland, Ohio 44135

10. Work Unit No.: 128-31
11. Contract or Grant No.:

12. Sponsoring Agency Name and Address
National Aeronautics and Space Administration
Washington, D. C. 20546

13. Type of Report and Period Covered: Technical Note
14. Sponsoring Agency Code:

15. Supplementary Notes

16. Abstract

Approximate analytical expressions are derived for the response of a vaporization limited combustion process to acoustic oscillations which have distorted wave shapes. Some exact numerical solutions are presented for comparison. The response is shown to be dependent on the type of distortion. For some conditions the response is an order of magnitude larger than that for sinusoidal wave shapes. The results imply that wave distortion could cause unstable combustion and should be considered in the design of rocket and jet engine combustors.

17. Key Words (Suggested by Author(s))	18. Distribution Statement
Dynamic response Rocket combustion Drop vaporization Combustion instability Nonlinear response	Unclassified - unlimited

19. Security Classif. (of this report)	20. Security Classif. (of this page)	21. No. of Pages	22. Price*
Unclassified	Unclassified	39	$3.00

*For sale by the Clearinghouse for Federal Scientific and Technical Information
Springfield, Virginia 22151

AMPLIFICATION BY WAVE DISTORTION OF THE DYNAMIC RESPONSE OF VAPORIZATION LIMITED COMBUSTION

by Marcus F. Heidmann

Lewis Research Center

SUMMARY

The response of a combustion process to acoustic oscillations which have distorted wave shapes is analyzed. A combustion process where burning rate is proportional to an exponential power of a Reynolds number is assumed, and specific application is made to drop vaporization in rocket combustors.

Analytical solutions are derived for the in-phase and out-of-phase response factors (components of the burning rate in-phase and out-of-phase with pressure). The response is shown to depend on the harmonic coefficients and phase angles in the Fourier series used to describe distorted wave shapes. The analytical solutions are compared with exact numerical evaluations.

The addition of harmonic content to acoustic oscillations can increase the in-phase response factor by an order of magnitude above that for sinusoidal wave shapes. The largest increase occurs when the harmonic components and acoustic particle velocities are all in-phase. The out-of-phase response is zero for this condition, but with phase shifts it has a finite value.

The effects of wave distortion on the response factors depend on the relative axial velocity of vaporizing drops. Large effects are observed when relative velocities are less than about 30 meters per second or 500 feet per second.

INTRODUCTION

Nonlinear instability limits of rocket engine combustors are one of the least understood properties of unstable combustion. These limits are usually established by exploding bombs of various sizes within the combustor. The engine remains stable to a bomb disturbance below some threshold level, and self-sustained instability is triggered above that level. Although simple in concept, such stability rating has uncertainties.

Bomb size alone is not the only variable. The type of bomb and its location also affect the results. In addition, instability is occasionally triggered by a bomb which normally does not cause instability, or it can be self-triggered by the combustion without bombs. The cause of instability and the variables affecting the stability limits are of vital concern in the design of high performance rocket engines.

The purpose of this study is to demonstrate the importance of wave distortion to both the analysis of instability and to the design of stable combustors. Distorted waves (pressure wave shapes which depart from pure sinusoidal forms) are generated by the bombs that trigger instability. Also, distorted wave shapes are usually observed during acoustic mode instability. The distortion usually increases with the amplitude of the oscillations. In the limit a shock wave or other highly nonsinusoidal wave form develops. Wave distortion, however, is not limited to high amplitudes. Instability in some engines exhibits simultaneous resonance of several acoustic modes - usually at harmonic frequencies - and distorted wave shapes are seen at very low amplitudes.

The effect of wave distortion on the acoustic amplification that can be expected from a drop vaporization process is examined. Steady combustion in liquid rockets is usually assumed to be vaporization limited, and the quantitative agreement between theory and experiment has been good (ref. 1). Vaporization-limited combustion is also expected for nonsteady combustion. Although this has been qualitatively confirmed, there are quantitative deficiencies in theoretical analyses of the problem. Dynamic analyses of the vaporization process (refs. 2 and 3) show an acoustic gain that is insufficient to overcome acoustic losses and cause instability. Acoustic oscillations with sinusoidal wave shapes were assumed in the previous studies; wave distortion was neglected.

The importance of wave distortion in unstable combustion was first observed in studies with numerical models of the type developed by Priem and Guentert (ref. 4). These two-dimensional model studies of the combustor (both the combustion mechanism and the gas dynamics are modeled) show that a drop-vaporization process can support unstable combustion. An explanation of the result is not obvious, and the validity of the result could be questioned. However, examining the detailed numerical computations showed that wave distortion could be very important. Although a sinusoidal disturbance is initially introduced, the pressure-time histories presented in references 4 and 5 show that this property is quickly lost and that the instability develops and grows into a distorted wave form. Acoustic gains extracted from the distorted-wave instability in reference 5 are about three times larger than those obtained from the dynamic response of the same vaporization process to sinusoidal oscillations. These observations prompted the present study.

A vaporization model where burning rate is simply related to some power of the drop Reynolds number is used. As such, the model generally characterizes convective heat- and mass-transfer processes, and the results are qualitatively applicable to a variety of

combustion mechanisms. This study, however, is specifically directed toward drop vaporization.

The open-loop response of the vaporization process to a variety of wave shapes is analyzed. Approximate analytical expressions are derived for both the in-phase and out-of-phase response factors (components of the burning rate in-phase and out-of-phase with the pressure oscillation). Solutions for some specific conditions of wave distortion are presented, and the probable effect on unstable combustion is discussed. Exact solutions obtained by numerical techniques are also presented. They show the precision obtained by the theoretical approach. Some of these numerical results have previously appeared in reference 6.

OPEN-LOOP MODEL

The open-loop response of an assumed combustion process will be used to predict the acoustic amplification of the process within an unstable combustor. In such open-loop analyses the perturbation in burning rate caused by assumed acoustic oscillations are evaluated. The response of the process is obtained by comparing the output (burning rate) with the input (acoustic oscillations).

Combustion Process

Precise modeling of a specific combustion process is not intended or necessary for the purpose of this analysis. It will be shown that a combustion process where burning rate (mass or energy release rate per unit volume), simply given by

$$w = C_1(\mathrm{Re})^m = C_1\left(\frac{\rho DU}{\mu}\right)^m \tag{1}$$

is a functional relation particularly sensitive to wave distortion. (Symbols are defined in appendix A.)

A Reynolds number dependency (eq. (1)) characterizes the convective heat- and mass-transfer processes that dominate many combustion mechanisms. Among these are the erosive burning of solid propellants and drop vaporization in liquid rockets and jet engines. Drop vaporization is particularly dominated by such Reynolds number dependence, and it will be emphasized in this analysis. For drop vaporization the burning rate is usually proportional to the one-half power of the drop Reynolds number, $m = 1/2$.

Priem and Guentert (ref. 4) used a vaporization model equivalent to that given by

equation (1) to obtain their useful correlations for nonlinear instability limits of liquid rockets. The approach they originally used will be followed. The gas viscosity μ and the drop diameter D will be assumed to be constant.

The relative velocity U in the Reynolds number (eq. (1)) introduces an important distortion-sensitive parameter. For an axially moving drop in a cylindrical chamber, U is the magnitude of the relative velocity vector given by

$$U^2 = |u_l - u_z|^2 + u_\theta^2 + u_r^2 \tag{2}$$

Gas velocity oscillations in any of three vector directions affect the burning rate. Because of the greater interest in transverse-mode instability in rocket combustors, this analysis will be restricted to transverse-velocity oscillations. The axial-velocity difference $|u_l - u_z|$ is assumed to be constant. For simplicity, the transverse velocities are combined into a single transverse-velocity vector u_t giving

$$U = \overline{\Delta V}\left[1 + \left(\frac{u_t}{\overline{\Delta V}}\right)^2\right]^{1/2} \tag{3}$$

where

$$\overline{\Delta V} = |u_l - u_z|$$

$$u_t^2 = u_\theta^2 + u_r^2$$

When a perturbed gas density is defined as $\rho = \bar{\rho}(1 + \rho')$, a burning rate normalized by the burning rate without oscillations w/w_0 can be expressed as

$$W = \frac{w}{w_0} = (1 + \rho')^m \left[1 + \left(\frac{u_t}{\overline{\Delta V}}\right)^2\right]^{m/2} \tag{4}$$

where

$$w_0 = C_1\left(\frac{\rho D\ \overline{\Delta V}}{\mu}\right)^m$$

Equation (4) specifies the burning rate for any assumed transverse acoustic oscillation. As in reference 4, the process as modeled is insensitive to the frequency of the oscillation.

Actually, the response of the vaporization process is frequency dependent (refs. 2 and 3). Figure 1 shows a typical response to sinusoidal oscillations. (Response is defined on p. 6.) The peak value of the response denotes the most unstable condition. This peak value depends on the Reynolds number sensitivity of the process and is proportional to the exponential power of the drop Reynolds number. Oscillations in drop diameter reduce the response at low frequencies, and oscillations in drop temperature reduce it at high frequencies. Without these frequency-dependent properties, this analysis will only show how this frequency-response curve is modified by wave distortion. It will show how much the response, particularly the peak value, could be amplified or attenuated by distortion waves.

Acoustic Oscillations

The acoustic oscillations assumed for this analysis are given by

$$P' = \sum_{n=1}^{\infty} p_n \cos(n\omega t - \varphi_n)$$

$$\rho' = \sum_{n=1}^{\infty} \rho_n \cos(n\omega t - \varphi_n)$$

$$u_t = \sum_{n=1}^{\infty} cu_n \cos(n\omega t - \varphi_n - \theta_n) \tag{5}$$

The oscillating gas properties are expressed as Fourier series which can describe any wave shape. The phase angle φ_n specifies the phase relation between harmonic components. This harmonic phase angle is assumed to be identical for pressure and density, an approximation that is reasonably realistic. The gas velocity expression also contains this harmonic phase angle but is further modified by a velocity phase angle θ_n. This velocity phase angle specifies the velocity-pressure phase relations. When θ_n is zero, the velocity and pressure are in-phase, and traveling wave properties are simulated. For standing acoustic modes, the velocity and pressure are out of phase; a

θ_n of 90^o simulates this condition. Some acoustic modes exhibit neither pure traveling or standing properties.

Response

Imposing the acoustic oscillations expressed as harmonic series on the combustion process causes a perturbation in the burning rate that can also be expressed as a harmonic series. An important parameter obtained from a comparison of such burning-rate oscillations with the acoustic oscillations is the portion of the burning rate that is in phase with the pressure oscillations. Based on the Rayleigh criterion for heat driven waves, this in-phase component gages with the ability of the process to drive the acoustic oscillations.

The in-phase component of the burning rate will be called the nonlinear in-phase response factor, $\mathcal{R}_{n\ell}$. It can be extracted from the burning rate and normalized by a correlation procedure (ref. 2) defined by

$$\mathcal{R}_{n\ell} = \frac{\int_0^{2\pi} W' P' d\omega t}{\int_0^{2\pi} (P')^2 d\omega t} \tag{6}$$

For rocket combustors, in-phase response factors greater than some value between 0.8 and 1.0 will usually denote unstable combustion for sinusoidal oscillations; that is, the oscillations will grow with time. Whether the same critical values apply to the growth of distorted waves has not been rigorously established. Intuition and an examination of the distorted wave instability with the Priem-Guentert model indicate that the same critical values apply. Without analytical proof at this time, a nonlinear in-phase response factor $\mathcal{R}_{n\ell}$ of 0.8 to 1.0 will be assumed to discriminate between stable and unstable combustion.

The portion of the burning rate that is out-of-phase with pressure is also important in combustor stability studies with sinusoidal waves. This out-of-phase component largely effects only the frequency of an unstable combustor. However, the exact role and definition of an out-of-phase response factor for distorted waves also lacks analytical treatment.

The nonlinear out-of-phase response factor $\mathcal{I}_{n\ell}$ defined by

$$\mathcal{I}_{n\ell} = \frac{\int_0^{2\pi} W' \sum_{n=1}^{\infty} p_n \sin(n\omega t - \varphi_n) d\omega t}{\int_0^{2\pi} (P')^2 d\omega t} \tag{7}$$

will be used. The definition is similar to that used for sinusoidal waves. This nonlinear out-of-phase response factor $\mathcal{I}_{n\ell}$ together with the nonlinear in-phase response factor $\mathcal{R}_{n\ell}$ are considered to be an adequate characterization of the response of a process to distorted acoustic oscillations.

Response factors can be used in the linear analysis of combustor stability to precisely couple the combustion process to the gas dynamics. In linear analyses, where all oscillations have sinusoidal wave shapes, the relationship

$$W' = (\mathcal{R} + i\mathcal{I})P' \tag{8}$$

exactly specifies the coupling.

When distorted-gas dynamic waves cause distorted burning-rate perturbations, a precise coupling relation has not been established. However, approximate relations can be formulated. This study is directed toward the approximation given by

$$W' = (\mathcal{R}_{n\ell} + i\mathcal{I}_{n\ell})P' + \text{residuals}$$

$$= (\mathcal{R}_{n\ell} + i\mathcal{I}_{n\ell})\left[p_1 \cos(\omega t - \varphi_1) + p_2 \cos(2\omega t - \varphi_2) + \ldots + p_n \cos(n\omega t - \varphi_n)\right] + \text{residuals} \tag{9}$$

With this approximation, the coupling is established by the two nonlinear response factors $\mathcal{R}_{n\ell}$ and $\mathcal{I}_{n\ell}$, which will be discussed throughout this report.

These nonlinear response factors are in fact weighted averages of harmonic response factors that can be specified for each harmonic component of the acoustic oscillations. For example, the nonlinear in-phase response factor given by equation (6) can be shown to be equivalent to an average of the harmonic response factors given by

$$\mathcal{R}_{n\ell} = \frac{p_1^2\mathcal{R}_1 + p_2^2\mathcal{R}_2 + \ldots + p_n^2\mathcal{R}_n}{p_1^2 + p_2^2 + \ldots + p_n^2} \tag{10}$$

where the harmonic response factors $\Re_n$ are specified by

$$\Re_n = \frac{\int_0^{2\pi} W' p_n \cos(n\omega t - \varphi_n)\, d\omega t}{\int_0^{2\pi} \left[p_n \cos(n\omega t - \varphi_n)\right]^2 d\omega t} \tag{11}$$

Another approximate coupling relationship, formulated by conventional methods of harmonic ordering, weighs the harmonic response factors in a different manner. The relationship formulated by such methods is

$$W' = (\Re_1 + i\mathcal{I}_1)p_1 \cos(\omega t - \varphi_1) + (\Re_2 + i\mathcal{I}_2)p_2 \cos(2\omega t - \varphi_2) + \ldots$$

$$+ (\Re_n + i\mathcal{I}_n)p_n \cos(n\omega t - \varphi_n) + \text{residuals} \tag{12}$$

With this approximation a series of harmonic response factors must be specified to establish the coupling between the gas dynamics and the combustion process. (A discussion of the harmonic response factors is given in appendix B.)

There is no rigorous justification for the use of either of the coupling relationships presented, and others could also be formulated. The degree of precision obtained by any approximation will depend on the specific application and the method of handling the residuals.

THEORETICAL SOLUTIONS

The method used to obtain analytical solutions for the nonlinear response factors will be described. A general solution will be derived. The composition of the general solution and the reasons for the effect of distortion variables on response will be discussed.

Some additional simplifying assumptions will be made to describe the acoustic oscillations. With these assumptions analytical solutions having greater utility are obtained. These solutions will be used in the RESULTS AND DISCUSSION section to describe the effect of some specific variations in wave distortion on the response factor.

General Solution and Discussion

Analytical solutions for the response factors were obtained by assuming exponential notations to simplify the mathematical procedures. The burning-rate expression (eq. (4)) combined with the assumed acoustic oscillations (eq. (5)) gives

$$W = \left[1 + \sum_{n=1}^{\infty} \frac{\rho_n}{2} e^{i(n\omega t - \varphi_n)} + \frac{\rho_n}{2} e^{-i(n\omega t - \varphi_n)}\right]^m \times \left\{1 + \left[\sum_{n=1}^{\infty} \frac{u_n}{2} e^{i(n\omega t - \varphi_n - \theta_n)} + \frac{u_n}{2} e^{-i(n\omega t - \varphi_n - \theta_n)}\right]^2\right\}^{m/2} \quad (13)$$

Two radical terms appear in equation (13). Each was separately expanded by a Taylor series. However, the squaring of the harmonic function in the radical term on the right was performed before the expansion. Both radical terms were expanded about their time invariant quantities, and only the first terms of the expansions were used.

Multiplying the two expansions as indicated by equation (13) gives an expression for the burning rate of the form

$$W = \overline{W}(1 + W') \quad (15)$$

The perturbation in burning rate W' can be arranged in harmonic series given by

$$W' = \sum_{n=1}^{\infty} \sum_{r=1}^{\infty} A_{n,r} \left[e^{i(n\omega t + \alpha_{n,r})} + e^{-i(n\omega t + \alpha_{n,r})}\right] \quad (16)$$

which is of the same form as the pressure perturbation

$$P' = \sum_{n=1}^{\infty} \frac{p_n}{2} \left[e^{i(n\omega t - \varphi_n)} + e^{-i(n\omega t - \varphi_n)}\right]$$

In equation (16) the $A_{n,r}$ terms are generated by the cross product of the pressure and velocity coefficients p_n and u_n. The $\alpha_{n,r}$ terms are sums and differences of the harmonic and velocity-pressure phase angles φ_n and θ_n.

The nonlinear in-phase response factor $\mathcal{R}_{nl}$ is obtained by performing the integration indicated by equation (7), which involves the product W'P'. Performing the integration gives

$$\mathcal{R}_{nl} = \frac{\sum_{n=1}^{\infty}\sum_{r=1}^{\infty} \frac{p_n}{2} A_{n,r} \left[e^{\alpha_{n,r}-\varphi_n} + e^{-(\alpha_{n,r}-\varphi_n)}\right]}{\sum_{n=1}^{\infty} p_n^2} \tag{17}$$

which can also be expressed as

$$\mathcal{R}_{nl} = \frac{\sum_{n=1}^{\infty}\sum_{r=1}^{\infty} p_n A_{n,r} \cos(\alpha_{n,r} - \varphi_n)}{\sum_{n=1}^{\infty} p_n^2} \tag{18}$$

A solution for $\mathcal{R}_{nl}$ where acoustic properties higher than the second order in harmonic content and cross products of harmonic coefficients higher than fourth order are neglected is given by

$$\mathcal{R}_{nl} = m\left(\overbrace{\frac{\rho_1 p_1 + \rho_2 p_2}{p_1^2 + p_2^2}}^{1} + \frac{1}{2}\left(\frac{c}{\overline{\Delta V}}\right)^2 \left\{ \frac{\overbrace{p_1 u_1 u_2 \cos(\varphi_2 + \theta_2 - \theta_1)}^{2} + \overbrace{\frac{1}{2} p_2 u_1^2 \cos(2\theta_1 - \varphi_2)}^{3} + \overbrace{m(\rho_1 p_1 + \rho_2 p_2) u_1 u_2 \cos\theta_1 \cos\theta_2}^{4} + \overbrace{\frac{m}{4}\rho_1 p_1 u_1^2 \cos 2\theta_1}^{5} + \overbrace{\frac{m}{4}\rho_2 p_2 u_2^2 \cos 2\theta_2}^{6}}{\underbrace{\left(p_1^2 + p_2^2\right)}^{7}\underbrace{\left[1 + \frac{1}{2}\left(\frac{c}{\overline{\Delta V}}\right)^2 \left(u_1^2 + u_2^2\right)\right]}_{8}} \right\}\right) \tag{19}$$

In this solution $\varphi_1 = 0$ has been assumed; that is, all phase angles have been referenced to the first harmonic pressure oscillations.

Some qualitative interpretations of equation (19) are possible. The response is basically proportional to the exponent m on the Reynold's number in the burning-rate expression. The solution consists of two major divisions: term 1 and terms 2 to 8. Term 1 is comparable to the solution obtained by linear (sinusoidal perturbation) analy-

sis. Its value is close to one and it is insensitive to variations in acoustic properties when $\rho_n = \frac{1}{\gamma} p_n$.

The terms within the bracket are the primary contributions of wave distortion to the response. Their effect on the response factor increases with a decrease in the steady axial-velocity difference $\overline{\Delta V}$. All these terms depend on the phase relations used to describe wave distortion. Maximum values are obtained for zero phase angles (i.e., velocity in-phase with pressure and no phase displacement between harmonic components). The response factor is amplified by wave distortion for such in-phase acoustic properties. Attentuation occurs for certain combinations of phase angles that give large negative values for the cosine functions.

Terms 2 and 3 are the major contributions of wave distortion to the response because of their lower order in cross products of the coefficients. Term 2 arises because the product of the first- and second-harmonic velocity components produces a first-harmonic component in the burning rate. This harmonic can be in-phase with the first-harmonic component of the pressure oscillation. In term 3 the square of the first harmonic terms of the velocity produces second-harmonic burning-rate components, which can correlate with the second-harmonic pressure component. Terms 4 to 6, although high order, can be interpreted in a similar manner. Although not so arranged, equation (19) is composed of first- and second-harmonic responses $\Re_1$ and $\Re_2$, which combine to give the nonlinear in-phase response $\Re_{nl}$. The contributions to $\Re_1$ and $\Re_2$ can be recognized by the respective pressure coefficients p_1 and p_2 appearing in terms 2 to 6. (Appendix B gives solutions for $\Re_1$ and $\Re_2$.)

Terms 7 and 8 can be considered to be normalizing factors. Term 7 arises from the numerator in equation (7) and is basically the square of the rms pressure oscillation. Term 8 is related to the mean value of the burning rate, where

$$\overline{W} = \left[1 + \frac{1}{2}\left(\frac{c}{\overline{\Delta V}}\right)^2 \left(u_1^2 + u_2^2\right)\right]^{m/2}$$

The mean burning rate and term 8 increase with an increase in the amplitude of the velocity oscillations, but is independent of the pressure amplitude.

Specific Solution

The general solution given by equation (19) can be expressed in a form that is more conveniently used to examine some specific oscillating conditions. Some interrelations between acoustic gas properties are assumed for this purpose. The gas density perturbations are assumed to be proportional to the pressure perturbations such that

$\gamma\rho_n = p_n$. This equation is usually valid only for small perturbations. Also, the coefficients of the gas velocity expressions are assumed to be proportional to the pressure such that $\gamma u_n = J_n p_n$. This is also adopted from small perturbation theory. The proportionality constant J_n is equal to one for weak traveling waves.

With these restrictions and definitions and making specific application to drop vaporization where $m = 1/2$, equation (19) becomes

$$\mathcal{R}_{nl} = \frac{1}{2\gamma} + \frac{\frac{1}{2}\left(\frac{cJ_1}{\overline{\Delta V}}\right)^2\left(\frac{p_1}{\gamma}\right)^2}{1+\left(\frac{p_2}{p_1}\right)^2}\left\{\frac{\frac{\gamma}{p_1}\left(\frac{p_2}{p_1}\right)\left[\frac{J_2}{J_1}\cos(\varphi_2+\theta_2-\theta_1)+\frac{1}{2}\cos(2\theta_1-\varphi_2)\right]+\frac{1}{2}\frac{J_2}{J_1}\left(\frac{p_2}{p_1}\right)^2\cos\theta_1\cos\theta_2+\frac{1}{8}\cos 2\theta_1+\frac{1}{8}\left(\frac{J_2}{J_1}\right)^2\left(\frac{p_2}{p_1}\right)^4\cos 2\theta_2}{1+\frac{1}{2}\left(\frac{cJ_1}{\overline{\Delta V}}\right)^2\left(\frac{p_1}{\gamma}\right)^2\left[1+\left(\frac{J_2}{J_1}\right)^2\left(\frac{p_2}{p_1}\right)^2\right]}\right\} \quad (20)$$

Evaluations of equation (20) are used in the RESULT AND DISCUSSION to examine the effect of wave distortion on the response.

A solution for the nonlinear out-of-phase response $\mathcal{I}_{nl}$ can be obtained by a method similar to that used for the $\mathcal{R}_{nl}$ solution. The result for $\gamma\rho_n = p_n$, $\gamma u_n = J_n p_n$, and $m = 1/2$, a solution comparable to equation (20), is

$$\mathcal{I}_{nl} = \frac{1}{2\gamma} + \frac{\frac{1}{2}\left(\frac{cJ_1}{\overline{\Delta V}}\right)^2\left(\frac{p_1}{\gamma}\right)^2}{1+\left(\frac{p_2}{p_1}\right)^2}\left\{\frac{\frac{\gamma}{p_1}\left(\frac{p_2}{p_1}\right)\left[\frac{J_2}{J_1}\sin(\varphi_2+\theta_2-\theta_1)+\frac{1}{2}\sin(2\theta_1-\varphi_2)\right]+\frac{1}{2}\frac{J_2}{J_1}\left(\frac{p_2}{p_1}\right)^2\sin(\theta_2-\theta_1)+\frac{1}{8}\sin 2\theta_1+\frac{1}{8}\frac{J_2}{J_1}\left(\frac{p_2}{p_1}\right)^4\sin 2\theta_2}{1+\frac{1}{2}\left(\frac{cJ_1}{\overline{\Delta V}}\right)^2\left(\frac{p_1}{\gamma}\right)^2\left[1+\left(\frac{J_2}{J_1}\right)^2\left(\frac{p_2}{p_1}\right)^2\right]}\right\} \quad (21)$$

This out-of-phase response is zero when the phase angles are zero, that is, when pressure-velocity and the harmonic components are all in-phase. At other phase angles it varies inversely with the relative axial gas velocity, $\overline{\Delta V}$. Most of the terms in equation (21) are similar to those for $\mathcal{R}_{nl}$ in equation (20) except for a sine and cosine interchange of the phase angle functions. This comparison of equations (20) and (21) shows that a change in the in-phase property of a burning-rate perturbation causes a complimentary change in the out-of-phase property.

NUMERICAL SOLUTIONS

The analytical solutions for the response factors derived in the previous section are approximate because (1) Taylor series expansions were used and (2) some higher order

cross products of coefficients were neglected. Exact solutions, which do not have these limitations, were obtained by numerical techniques for the conditions described in the RESULTS AND DISCUSSION section. These exact solutions, when compared with the analytical solutions, show the overall precision of the more readily evaluated analytical expressions.

Numerical solutions were obtained by programming the burning rate, the acoustic oscillations, and the response expression for exact solutions on a digital computer. The solutions were restricted to the conditions that apply to the analytical solutions given by equations (20) and (21). The expressions used are as follows:

Burning rate -

$$W = (1 + \rho')^{1/2} \left[1 + \left(\frac{u_t}{\overline{\Delta V}} \right)^2 \right]^{1/4}$$

Acoustic oscillations -

$$P' = p_1 \left[\cos \omega t + \frac{p_2}{p_1} \cos(2\omega t - \varphi_2) \right]$$

$$\rho' = \frac{p'}{\gamma} \left[\cos \omega t + \frac{p_2}{p_1} \cos(2\omega t - \varphi_2) \right]$$

$$u_t = \frac{cJ_1 p_1}{\gamma} \left[\cos(\omega t - \theta_1) + \frac{J_2}{J_1} \frac{p_2}{p_1} \cos(2\omega t - \varphi_2 - \theta_2) \right]$$

Numerical integration of equations (7) and (10) gave the response factors $\mathcal{R}_{n\ell}$ and $\mathcal{I}_{n\ell}$.

RESULTS AND DISCUSSION

The results to be shown and discussed will be those for a combustion process where $w \approx (Re)^{1/2}$. This process applies most directly to drop vaporization in rocket combustors. The variables which describe the distortion of acoustic oscillation will be examined. Generally, the independent effect of wave distortion variables on the response of the process will be shown. The purpose of the discussion is to demonstrate the importance of wave distortion in unstable combustion.

Harmonic Content

The effect of varying the amount of second harmonic content on the nonlinear in-phase response $\Re_{n\ell}$ is shown in figure 2. The effect on pressure wave shape is also shown. For the conditions of figure 2 all the phase angles are zero; that is, there is no phase displacement between harmonic components and a velocity in-phase with pressure and density. The relative axial Mach number term $\overline{\Delta V}/cJ_1$ is 0.02, which is a relative drop velocity in rocket combustors of about 30 meters per second (100 ft/sec).

The in-phase response exhibits optimum properties as a function of both pressure amplitude and second harmonic contents. Maximum response occurs at an amplitude of about 0.02 for a second-harmonic to first-harmonic amplitude ratio of about 0.8. One of the reasons for the low response at higher amplitudes is the increase in mean burning rate with amplitude. Increasing the mean decreases the relative size of a perturbation and reduces the response (see appendix C for mean values).

The significance of the response values shown in figure 2 can be gaged by a comparison with the $p_2/p_1 = 0$ curve in figure 2. The $p_2/p_1 = 0$ curve is the response to sinusoidal waves and is shown to be relatively insensitive to pressure amplitude. The response is about $1/2\gamma$ (the value obtained by linear analysis), which is too low to cause instability in rocket combustors. Thus, distorting the acoustic oscillations with second-harmonic content can amplify the response by a factor of 10 above this linear value. The response is much larger than that needed for instability (i.e., $\Re_{n\ell}$ is greater than 0.8 to 1.0.) The contribution of the harmonic response factors $\Re_1$ and $\Re_2$ to the overall nonlinear response $\Re_{n\ell}$ is discussed in appendix B.

For the conditions shown in figure 2, maximum amplification occurs at the relatively low oscillation pressure amplitude of 0.02. This amplitude is comparable to the usual combustion noise in rocket engines. It is possible that combustion instability could develop from distorted acoustic oscillations buried within the usual noise spectrum of the engine.

A comparison of the analytical and numerical results in figure 2 shows that the analytical solutions overpredict the response by about 10 to 20 percent. The functional form of the solution, however, appears to be correct.

Some types of wave distortion are not adequately characterized by only two-harmonic components as discussed thus far in this report. This is particularly true for high-amplitude combustion oscillations where the wave shape becomes highly distorted. A high-amplitude wave shape of special interest in rocket-engine instability is that for the traveling transverse acoustic mode. High amplitudes for this mode are frequently observed during instability with large rocket engines.

The pressure wave for strong traveling acoustic modes has a characteristic shape which was experimentally examined and described in reference 7. The harmonic content

of increasingly higher orders was needed to characterize wave shapes for increasing amplitudes. The following relation approximated the behavior

$$P' = \sum_{n=1}^{\infty} p_1^n \cos n\omega t \tag{22}$$

where the maximum to minimum and mean pressure amplitudes are given by

$$P'_{max} - P'_{min} = \frac{2p_1}{1 - p_1^2} \tag{23}$$

and

$$P'_{rms} = \frac{p_1}{\sqrt{2(1 - p_1^2)}} \tag{24}$$

The following table shows the harmonic content and amplitudes:

p_1	p_2/p_1	p_3/p_1	p_4/p_1	$P'_{max} - P'_{min}$	P'_{rms}
0.01	0.01	0.0001	0.000001	0.02	0.0071
.1	.1	.01	.001	.201	.071
.3	.3	.09	.027	.66	.165
.5	.5	.25	.125	1.33	.41

Numerical solutions for the response factors were obtained for these waves. As previously, the assumptions that $\gamma\rho_n = p_n$, $\gamma u_n = J_n p_n$, and $J_n = 1.0$ were made. The results and typical pressure wave shapes are shown in figure 3. The response increases with amplitude and assymptotically reaches a maximum value of about 1.08. (The variation with relative velocity will be discussed later.) The response does not reach the peak value shown in figure 2 because the harmonic content for these waves is very small at the pressure amplitude of 0.02 where the peaks occur in figure 2. At this amplitude, p_2/p_1 is only 0.02 for these traveling mode waves. Also, the response does not fall at high amplitudes as in figure 2 because higher order harmonic components contribute to the response in this region (see appendix B). The maximum response of 1.08 (about

2.5 times the linear value) could cause unstable combustion. The harmonic distortion which grows with amplitude, therefore, is a potential cause of instability in rocket engines.

The results in figure 3 provide some insight into the causes for trigerable instability observed both experimentally and with the numerical model studies of Priem and Guentert (ref. 4). When disturbances of increasing amplitude are introduced in a combustor the harmonic content can be expected to grow with amplitude. At some amplitude there is sufficient harmonic content to give an in-phase response that can cause instability ($\Re_{n\ell}$ greater than 0.8 to 1.0). It appears that Priem and Guentert's numerical model studies depended on this amplification caused by wave distortion. It is probable that instability in rocket engines can be triggered by bomb pulses when they initiate oscillations with sufficient harmonic content.

Figure 3 also shows analytical results obtained from equation (20). The substitution $p_2 = (p_1)^2$ (from eq. (22)) was used and terms of a higher order than p_1^2 were neglected. This, together with the assumptions already stated, gives the result

$$\Re_{n\ell} = \frac{1}{2\gamma}\left[1 + \frac{\frac{1}{2}\left(\frac{cJ_1}{\overline{\Delta V}}\right)^2\left(\frac{p_1}{\gamma}\right)^2\left(\frac{3}{2}\gamma + \frac{1}{8}\right)}{1 + p_1^2 + \frac{1}{2}\left(\frac{cJ_1}{\overline{\Delta V}}\right)^2\left(\frac{p_1}{\gamma}\right)^2}\right] \tag{25}$$

This solution good to second order in harmonic content and amplitude coefficient agrees favorably with the exact solution for multiharmonic wave shapes. Some additional evaluations showed that deductions with regard to phase relations can also be made for these multiharmonic wave shapes on retaining angles in the derivation of equation (25). Also, a solution for $\measuredangle_{n\ell}$ for strong traveling waves can be deduced from equation (21).

Pressure-Velocity and Harmonic Phase Relations

The amplification caused by wave distortion depends on both the phase relation between the first- and second-harmonic components φ_n and the phase relations between pressure and velocity θ_n. The solutions for the response factors show that phase angle effects are not separable in either equation (20) for $\Re_{n\ell}$ or equation (21) for $\measuredangle_{n\ell}$. Many interacting effects are possible. The discussion of the phase relations will be limited to some of their gross effects.

The independent effect of the harmonic phase angle on the in-phase response factor $\Re_{n\ell}$ is shown in figures 4(a) and (b). The conditions are comparable to figure 2, but

only a second to first harmonic amplitude ratio of 0.2 is considered. The pressure-velocity phase angle is zero ($\theta_1 = \theta_2 = 0^o$). The in-phase response is shown to decrease for any phase shift between harmonic components. When the phase shift is 90^o, the response is reduced to near the linear value of $1/2\gamma$. Phase shifts of more than 90^o can give negative values of the in-phase response. Negative responses imply highly stable combustion.

Application of these harmonic phase-shift results to combustion instability is qualitative because the phase-shift properties of actual waves have received little attention. Steep-front or shock-like waves contain a second harmonic component which approaches a phase shift of 90^o. Such waves would not be as easily driven by the combustion process as are the strong symmetrical wave shapes shown in figure 3 where there is no harmonic phase shift. Phase shifts beyond 90^o seem improbable except for some types of multimode resonance. Any method of producing large harmonic phase shifts, however, should contribute to combustion stability.

The effect of harmonic phase shift on the out-of-phase response is shown in figures 4(c) and (d). Any phase shift between harmonic components causes an out-of-phase response. When the phase shift is positive, the response $\mathcal{J}_{n\ell}$ is positive; when the phase-shift is negative, $\mathcal{J}_{n\ell}$ is negative. The result is unusual because out-of-phase responses in linear analyses appear only for time-dependent processes. The significance of these out-of-phase responses from wave distortion remains to be established.

The independent effect of the velocity-pressure phase relation on the in-phase response is shown in figures 5(a) and (b). Any phase shift between pressure and velocity reduces the response, but the effect is much smaller than for a harmonic phase shift. The maximum reduction occurs for a 90^o phase shift, but the response remains above the linear value of $1/2\gamma$. A velocity out-of-phase with pressure ($\theta = 90^o$) characterizes standing mode resonance. The result implies that the standing mode resonance is not as easily driven as is the traveling mode resonance which exhibits in-phase velocity-pressure properties.

Any phase shift between pressure and velocity also causes an out-of-phase response $\mathcal{J}_{n\ell}$ to appear. This is shown in figures 5(c) and (d). The response is zero at 90^o increments rather than the 180^o increments found for the velocity-pressure angles in figure 4.

One condition of practical interest is an increase in the harmonic phase angle when the velocity-pressure phase angle is 90^o. This simulates the growth of shock-like waves in standing modes. The velocity is assumed to be out-of-phase with pressure ($\theta_1 = \theta_2 = 90^o$) because of the standing mode property. An increase in the phase angle between the harmonic components provides the wave steepening property. Figure 6 shows the effect on both $\mathcal{R}_{n\ell}$ and $\mathcal{J}_{n\ell}$. The effect of the harmonic phase angle on $\mathcal{R}_{n\ell}$ is similar to that when the pressure-velocity phase angle is zero (fig. 5). A harmonic

phase shift of 90^{o} (a limiting condition for shock-like waves) reduces the response to its linear value of $1/2\gamma$. Higher harmonic components should also be introduced for a complete solution for shock-like waves. It is concluded, however, that steepening the wave reduces the response, which in turn acts to limit the pressure amplitude; that is, a wave steepens when it grows in amplitude until the acoustic gains represented by the in-phase response match or equal the acoustic losses.

Relative Axial Velocity

The velocity sensitivity of a Reynolds number dependent process is the primary cause of the large changes in response with wave distortion. For drop vaporization this velocity sensitivity is controlled by the steady relative axial-drop velocity or Mach number $\overline{\Delta V}/c$. When this relative velocity is large, the vaporization rate is large. This makes the process relatively insensitive to velocity oscillations and any distortion of such oscillations.

The effect of the steady relative axial velocity on the in-phase response is shown in figure 7. For very large relative velocities, the response approaches the value of $1/2\gamma$ obtained by linear analysis. For the conditions used in figure 7, the amplification caused by wave distortion becomes appreciable only for relative axial Mach numbers less than about 0.1 (about 150 m/sec or 500 ft/sec in rocket combustors). However, Mach numbers below 0.1 typify drop vaporization in many rocket combustors, and a significant increase in response due to distortion can be expected.

The effect of the steady axial velocity is also shown in figure 3 which shows the in-phase response for strong traveling waves with multiple harmonic components. For these waves a decrease in the relative velocity decreases the pressure amplitude needed to obtain large response factors.

The relative axial velocity was one variable examined by Priem and Guentert (ref. 4) in their numerical model studies of instability. They showed that the size of the disturbance needed to start instability decreased with a decrease in relative velocity. The same result is implied by figure 3. The pressure amplitudes needed for instability ($\Re_{n\ell}$ greater than 0.8 to 1.0) decrease with a decrease in relative velocity.

The trend for large-scale liquid rockets is toward smaller contraction ratio designs which lead to higher relative axial Mach numbers. For example, an average $\overline{\Delta V}/C$ of about 0.15 characterizes drop vaporization in a relatively small contraction ratio combustor of 1.8. These smaller contraction ratio combustors should be more stable, but stability is not assured. As shown in figure 3, an increase in relative Mach number merely increases the pressure disturbance that the process can tolerate and still remain stable.

CONCLUDING REMARKS

This analysis using a simplified vaporization process has shown wave distortion to be an important variable in combustion stability. It can amplify the response of the process beyond that needed for unstable combustion and significantly affect stability predictions. This effect of wave distortion on stability should persist for a more precise vaporization model or for any combustion mechanism where Reynolds number is a dominant variable affecting combustion rate. It appears necessary to direct more attention to the causes and effects of wave distortion to obtain a complete understanding of the unstable combustion system.

Various deductions about combustor behavior can be made from this study and compared with experimental evidence. But such comparisons must be qualitative for several reasons. One, the analysis is incomplete. Only a simplified combustion process was examined, and no overall systems stability analysis was made. Two, conflicting experimental evidence is often found, or the independent effect of a particular parameter is not conclusively established. Recognizing these limitations, the following are of interest:

(1) Traveling mode resonance is more frequently encountered than standing mode resonance. - Acoustic gains are larger for the in-phase velocity-pressure properties of traveling waves than the out-of-phase properties of standing waves.

(2) Pressure amplitudes for traveling mode instability are usually larger than those for longitudinal standing mode instability. - Acoustic gains are reduced by the steepening of the wave shapes, which develops naturally in longitudinal modes at relatively low amplitudes.

(3) Disturbances above some finite amplitude can trigger unstable combustion. - Acoustic gains increase with the increase in harmonic distortion, which usually grows with amplitude.

(4) Large contraction ratio combustors are more prone to transverse mode instability than with low contraction ratios. - Acoustic gains from distorted waves are larger for the small relative axial drop velocities usually found in large contraction ratio combustors.

(5) Evidence of multimode resonance is common during the initial growth period of spontaneous instability. - Acoustic gains are large at low amplitudes for waves distorted by two harmonic components.

(6) Acoustic liners with broad-band tuning are most effective in suppressing instability. - A reduction in harmonic content (from broad-band tuning) may be more effective in reducing acoustic gains than reducing only the fundamental oscillation.

(7) The symmetrical wave shapes of traveling transverse mode instability tend to

steepen as they approach a limiting amplitude. - Acoustic gains decrease with wave steepening and eventually act to limit the amplitude.

SUMMARY OF RESULTS

The response of a combustion process to acoustic oscillations distorted by harmonic content was analyzed. A combustion process where burning rate is proportional to an exponential power of Reynolds number was assumed. Specific application was made to drop vaporization in rocket combustors where the exponential power is 1/2. The following results were obtained:

1. Analytical solutions were obtained for the in-phase and out-of-phase response factors (components of the burning rate in-phase and out-of-phase with the pressure oscillation, respectively). The solutions show the effects on the response factors of the harmonic amplitudes and phase relations, of the acoustic velocity amplitudes and velocity-pressure phase relation, and of a steady relative axial velocity. The analytical solutions show good agreement with exact numerical solutions.

2. Harmonic content can substantially increase the in-phase response factor. The addition of a second harmonic component to the acoustic oscillation can increase the response by an order of magnitude above that for sinusoidal oscillations. Higher order harmonic distortion (the type that normally grows with amplitude) can increase the in-phase response to 2.5 times the sinusoidal value.

3. The phase relation between harmonic components and the phase relation between velocity and pressure affect both the in-phase and out-of-phase response factors. The in-phase response factor is a maximum when both the harmonic components and the velocity-pressure are in-phase. No out-of-phase response exists for this condition. The in-phase response factor is less than the maximum when either the harmonic components or the velocity-pressure are phase shifted. With phase shifts, the out-of-phase response factor usually has a finite value. The effects of the harmonic component phase relation are larger than those for the velocity-pressure phase relation.

4. The relative axial velocity (of a burning drop in a combustor) controls the sensitivity of the process to wave distortion. Distortion effects on both response factors are significant when the relative axial Mach number is less than about 0.1.

5. Wave distortion is a crucial property affecting the response of the drop-vaporization process to acoustic oscillation. Changes in distortion can amplify or sup-

press the in-phase response factor and substantially affect the stability prediction of rocket combustors. Wave distortion should be carefully considered in the design of stable combustors.

Lewis Research Center,
National Aeronautics and Space Administration,
Cleveland, Ohio, January 6, 1971,
128-31.

APPENDIX A

SYMBOLS

$A_{n,r}$	harmonic coefficient for burning rate perturbations
C_1	proportionality constant
c	speed of sound
D	drop diameter
$\mathcal{I}_n, \mathcal{I}_{n\ell}$	out-of-phase response factor (harmonic and nonlinear)
J_n	proportionality constant in $\gamma u_n = J_n p_n$
m	Reynolds number exponent
n	harmonic order
P	pressure
P'_{rms}	rms pressure amplitude, $\left(\frac{1}{2}\sum_{n=1}^{\infty} p_n^2\right)^{1/2}$
p_n	harmonic coefficient for pressure perturbation
Re	Reynolds number
$\mathcal{R}_n, \mathcal{R}_{n\ell}$	in-phase response factor (harmonic and nonlinear)
t	time
U	magnitude of relative drop velocity vector
u_ℓ	axial velocity of drop
u_n	harmonic coefficient for transverse Mach number perturbations
u_z, u_θ, u_r	gas velocity (axial, tangential, and radial)
u_t	transverse velocity, $(u_\theta^2 + u_r^2)^{1/2}$
$\overline{\Delta V}$	relative velocity of drop, $\lvert u_\ell - u_z \rvert$
W	dimensionless burning rate
w	burning rate (energy release per unit time and volume)
w_o	initial burning rate without oscillations
$\alpha_{n,r}$	harmonic phase angle for burning rate perturbations
γ	ratio of specific heats
θ_n	harmonic phase angle for velocity-pressure relation
ρ	gas density
ρ_n	harmonic coefficients for density perturbation
φ_n	harmonic phase angle for pressure perturbations
μ	gas viscosity
ω	frequency
'	dimensionless perturbations, $x' = (x - \bar{x})/\bar{x}$
$\bar{}$	mean values

APPENDIX B

HARMONIC RESPONSE FACTORS

In this appendix harmonic response factors are presented for some representative conditions to show the magnitude of their contributions to the nonlinear response factor.

The expressions developed for the relation between the nonlinear and harmonic response factors (eqs. (8) and (11)) are

$$\mathcal{R}_{n\ell} = \frac{\sum_{n=1}^{\infty} (p_n)^2 \mathcal{R}_n}{\sum_{n=1}^{\infty} (p_n)^2} \tag{B1}$$

$$\mathcal{I}_{n\ell} = \frac{\sum_{n=1}^{\infty} (p_n)^2 \mathcal{I}_n}{\sum_{n=1}^{\infty} (p_n)^2} \tag{B2}$$

The nonlinear response factors are shown to be weighted averages of the harmonic response factors.

Both analytical and numerical solutions for the harmonic response factors were obtained. Analytical expressions for the first- and second-harmonic response factors were obtained by a method similar to that used for the nonlinear response factors. The expressions for $\gamma\rho_n = p_n$, $J_1 = J_2 = 1.0$, and $m = 1/2$ (comparable to eqs. (20) and (21) for the nonlinear response factors) are

$$\mathcal{R}_1 = \frac{1}{2\gamma}\left\{1 + \frac{1}{2}\left(\frac{cJ_1}{\overline{\Delta V}}\right)^2\left(\frac{p_1}{\gamma}\right)^2\left[\frac{\frac{\gamma}{p_1}\left(\frac{p_2}{p_1}\right)\left(\frac{J_2}{J_1}\right)\cos(\varphi_2 + \theta_2 - \theta_1) + \frac{1}{2}\left(\frac{p_2}{p_1}\right)^2\frac{J_2}{J_1}\cos\theta_2\cos\theta_1 + \frac{1}{8}\cos 2\theta_1}{1 + \frac{1}{2}\left(\frac{cJ_1}{\overline{\Delta V}}\right)^2\left(\frac{p_1}{\gamma}\right)^2\left[1 + \left(\frac{p_2}{p_1}\right)^2\left(\frac{J_2}{J_1}\right)^2\right]}\right]\right\} \tag{B3}$$

$$\mathcal{R}_2 = \frac{1}{2\gamma}\left\{1+\frac{1}{2}\left(\frac{cJ_1}{\overline{\Delta V}}\right)^2\left(\frac{p_1}{\gamma}\right)^2\left[\frac{\frac{\gamma}{p_1}\left(\frac{p_1}{p_2}\right)\cos(2\theta_1-\varphi_2)+\frac{1}{2}\frac{J_2}{J_1}\cos\theta_2\cos\theta_1+\frac{1}{8}\left(\frac{p_2}{p_1}\right)^2\left(\frac{J_2}{J_1}\right)^2\cos 2\theta_2}{1+\frac{1}{2}\left(\frac{cJ_1}{\overline{\Delta V}}\right)^2\left(\frac{p_1}{\gamma}\right)^2\quad 1+\left(\frac{p_2}{p_1}\right)^2\left(\frac{J_2}{J_1}\right)^2}\right]\right\} \tag{B4}$$

$$\mathcal{I}_1 = \frac{1}{4\gamma}\left(\frac{cJ_1}{\overline{\Delta V}}\right)^2\left(\frac{p_1}{\gamma}\right)^2\left[\frac{\frac{\gamma}{p_1}\left(\frac{p_2}{p_1}\right)\left(\frac{J_2}{J_1}\right)\sin(\varphi_2+\theta_2-\theta_1)+\frac{1}{2}\left(\frac{p_2}{p_1}\right)^2\frac{J_2}{J_1}\sin\theta_1\cos\theta_2+\frac{1}{8}\sin\alpha\theta_1}{1+\frac{1}{2}\left(\frac{cJ_1}{\overline{\Delta V}}\right)^2\left(\frac{p_2}{\gamma}\right)^2\left[1+\left(\frac{p_2}{p_1}\right)^2\left(\frac{J_2}{J_1}\right)^2\right]}\right] \tag{B5}$$

$$\mathcal{I}_2 = \frac{1}{8\gamma}\left(\frac{cJ_1}{\overline{\Delta V}}\right)^2\left(\frac{p_1}{\gamma}\right)^2\left[\frac{\frac{\gamma}{p_1}\left(\frac{p_1}{p_2}\right)\sin(2\theta_1-\varphi_2)+\frac{J_2}{J_1}\sin\theta_2\cos\theta_1+\frac{1}{4}\left(\frac{p_2}{p_1}\right)^2\left(\frac{J_2}{J_1}\right)^2\sin 2\theta_2}{1+\frac{1}{2}\left(\frac{cJ_1}{\overline{\Delta V}}\right)^2\left(\frac{p_1}{\gamma}\right)^2\left[1+\left(\frac{p_2}{p_1}\right)^2\left(\frac{J_2}{J_1}\right)^2\right]}\right] \tag{B6}$$

Figures 8(a) and (b) show the in-phase response factors $\mathcal{R}_1$, $\mathcal{R}_2$, and $\mathcal{R}_{nl}$ for the highest value curve in figure 2. For this condition the harmonic components and the velocity-pressure are in-phase, $(\overline{\Delta V}/cJ_1) = 0.02$ and $p_2/p_1 = 0.8$. Both the analytical and numerical solutions show $\mathcal{R}_1$ to be larger than $\mathcal{R}_{nl}$ and $\mathcal{R}_2$ smaller. For this case of a relatively large amount of second-harmonic content, the weighted averaging gives a nonlinear response factor that is smaller than the first harmonic response factor.

The relation between response factors are reversed when the second harmonic content is reduced. This is shown in figures 8(c) and (d) for $p_2/p_1 = 0.2$. The second-harmonic response factor is very large for this condition. This makes the nonlinear response larger than the first-harmonic response. The second-harmonic response is large because the process considered is a strong second-harmonic generator or frequency doubler (see appendix C). When the second-harmonic content of the acoustic oscillation is small, there is a strong correlation between the burning rate and this second-harmonic content. Increasing the second-harmonic content of the acoustic oscillation does not cause a proportional increase in the second-harmonic content of the burning

rate. This reduces the correlation and the second-harmonic response factor as observed in figures 8(c) and (d).

The out-of-phase response factors exhibit a behavior similar to that for the in-phase response factors. An example of one condition is shown in figure 9. This is comparable to figures 8(c) and (d) in that the second-harmonic response is much larger than the first-harmonic response. The weighted averaging gives a nonlinear response that is slightly higher than the first harmonic response.

Higher order response factors contribute to the nonlinear response for waves with multiple harmonic content. This is shown by the numerical solutions in figure 10 for strong traveling waves. As the pressure amplitude increases, higher order responses contribute to the nonlinear response and a constant value of nonlinear response is maintained at high amplitudes.

APPENDIX C

INSTANTANEOUS AND MEAN BURNING RATES

The burning rate, pressure, and acoustic velocity oscillations for a typical condition considered in this study are shown in figure 11. The burning-rate curve shows a large second-harmonic content even though the second-harmonic content of the acoustic oscillation is relatively small ($p_2/p_1 = 0.2$). The process is basically a harmonic generator or frequency doubler. This causes the burning rate to be highly distorted for any type of disturbance. When the pressure and velocity are not in phase (as in fig. 11), the burning rate curve on the average is not in phase with the pressure oscillation. Such burning rates have both in-phase and out-of-phase components with respect to the pressure oscillation and the respective response factors $\mathcal{R}_{nl}$ and $\mathcal{I}_{nl}$ assume finite values.

The mean burning rate of a drop vaporization or any Reynolds number dependent process generally increases in the presence of acoustic oscillations.

The analytical expression for the mean burning rate for drop vaporization is given by

$$\overline{W} = \left[1 + \frac{1}{2}\left(\frac{c}{\overline{\Delta V}}\right)^2 \left(u_1^2 + u_2^2\right)\right]^{1/4} \tag{C1}$$

For $\gamma u_n = J_n p_n$ and $\gamma \rho_n = p_n$, equation (C1) becomes

$$\overline{W} = \left\{1 + \frac{1}{2}\left(\frac{cJ_1}{\overline{\Delta V}}\right)^2 \left(\frac{p_1}{\gamma}\right)^2 \left[1 + \left(\frac{J_2}{J_1}\right)^2 \left(\frac{p_2}{p_1}\right)^2\right]\right\} \tag{C2}$$

The mean burning rate is primarily dependent on the relative axial velocity and pressure amplitude although large second-harmonic contents also affect the mean value.

The effect of relative velocity and amplitude is shown in figure 12 for $p_2/p_1 = 0.2$, $J_1 = J_2 = 1.0$, and $\gamma = 1.2$. The mean burning rate can more than double with an increase in pressure amplitude, and at low relative velocities the mean can increase by a factor of 5 or more. These increases in the mean with amplitude reduce the relative size of a given oscillation in burning rate and in part contribute to the decrease in response with amplitude shown in figures 2 and 4 to 7.

REFERENCES

1. Priem, Richard J.; and Heidmann, Marcus F.: Propellant Vaporization as a Design Criterion for Rocket-Engine Combustion Chambers. NASA TR R-67, 1960.

2. Heidmann, Marcus F.; and Wieber, Paul R.: Analysis of Frequency Response Characteristics of Propellant Vaporization. NASA TN D-3749, 1966.

3. Crocco, L.; Harrje, D. T.; Sirignano, W. A.; Bracco, F. V.; Mitchell, C. E.; Tang, P. K.; Williams, R. M.; Black, G. R.; and Stinger, W. A.: Nonlinear Aspects of Combustion Instability in Liquid Propellant Rocket Motors. Rep. AMS-SR-533g, Princeton Univ. (NASA CR-72270), June 1967.

4. Priem, Richard J.; and Guentert, Donald C.: Combustion Instability Limits Determined by a Nonlinear Theory and a One-Dimensional Model. NASA TN D-1409, 1962.

5. Kosvic, T. C.; Breen, B. P.; Levine, J.; and Coats, D. E.: Combustion Instability Response with Asymmetric Pressure Disturbances. Dynamic Science Corp. (NASA CR-72494), Jan. 1969.

6. Heidmann, M. F.: Amplification by Wave Distortion in Unstable Combustors. AIAA Journal, vol. 9, no. 2, Feb. 1971, p. 336.

7. Heidmann, Marcus F.: Empirical Characterization of Some Pressure Wave Shapes in Strong Traveling Transverse Acoustic Modes. NASA TM X-1716, 1969.

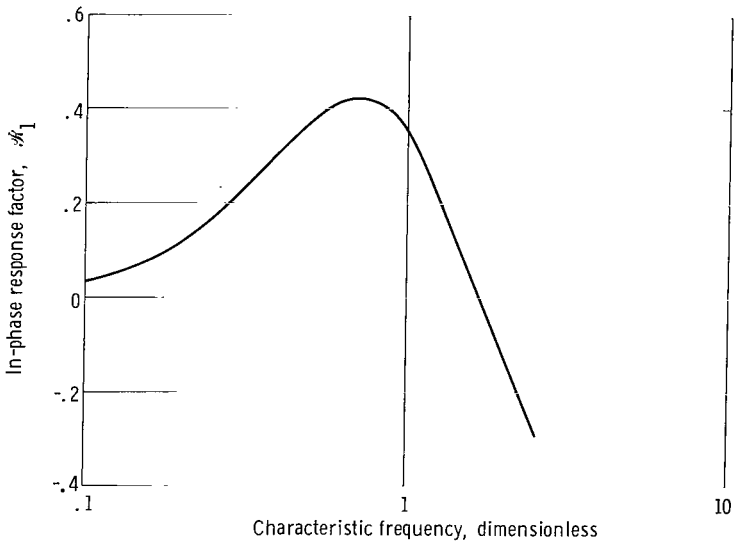

Figure 1. - Typical response of heptane drop vaporization to sinusoidal oscillations (ref. 1).

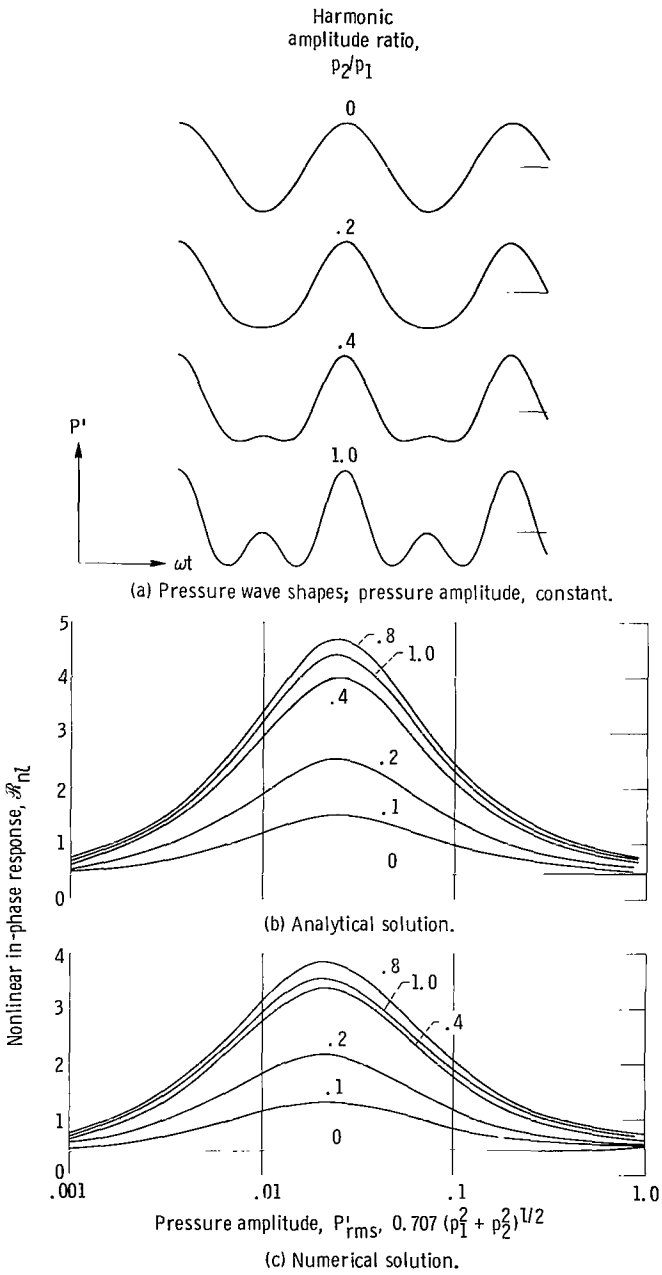

Figure 2. - Effect of amount of harmonic content on response and wave shape. Harmonic phase angle, $\varphi_2 = 0°$; velocity-pressure phase angles, $\theta_1 = \theta_2 = 0°$; relative axial Mach number, $\Delta V/cJ_1 = 0.02$; specific heat ratio, 1.2; proportionality constant, $J_2/J_1 = 1.0$.

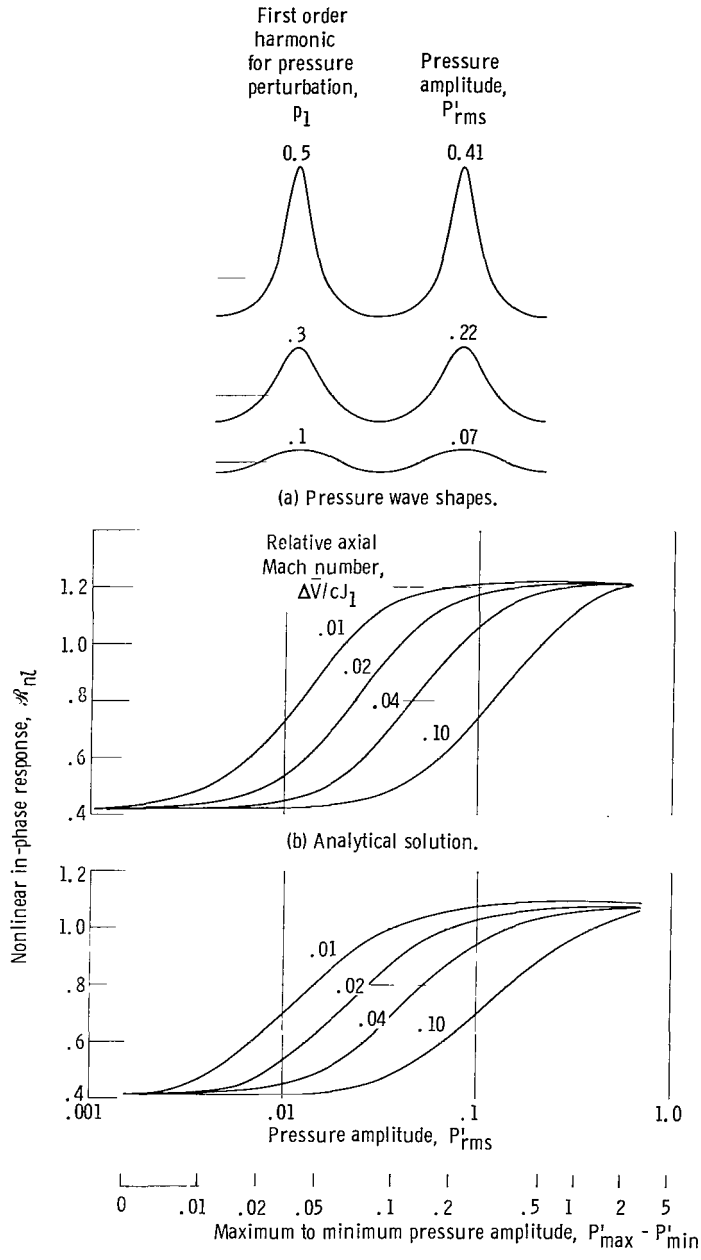

Figure 3. - Response and wave shapes for waves in strong traveling transverse acoustic modes.

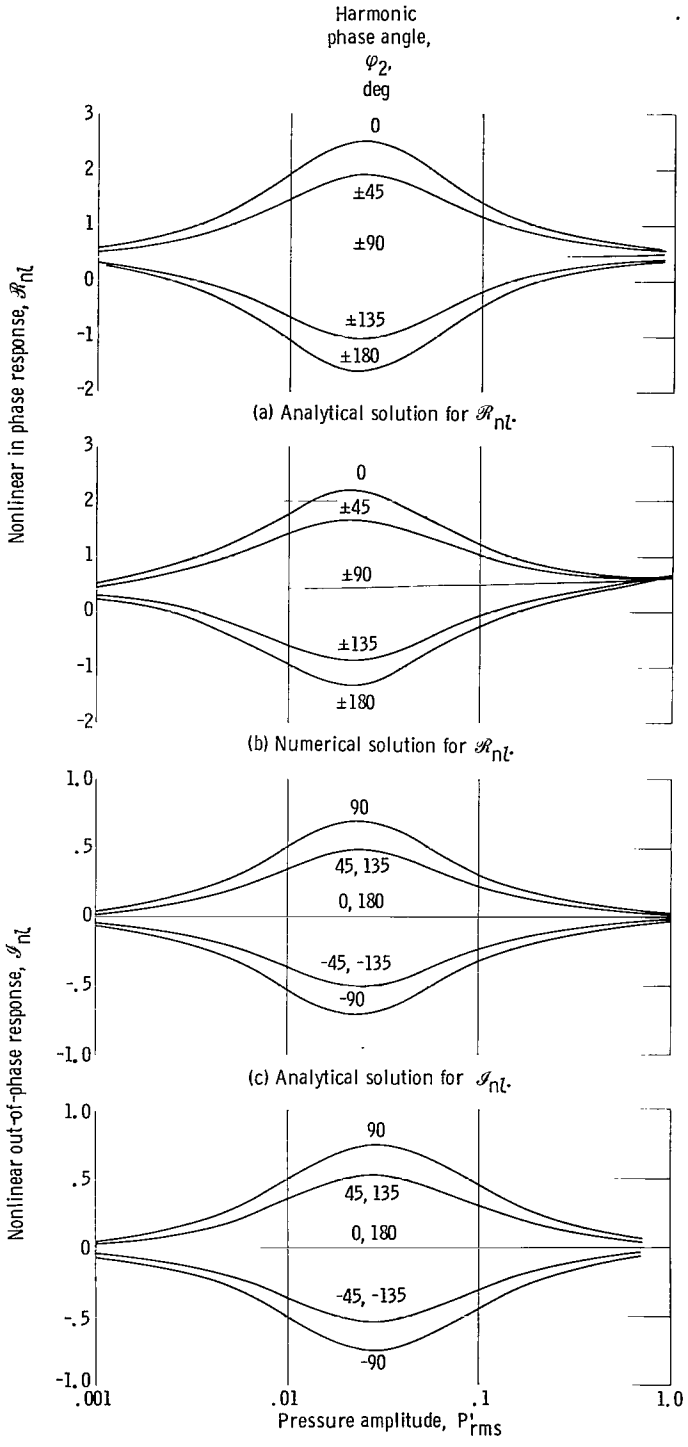

Figure 4. - Effect of harmonic phase angle on response. Relative axial Mach number, $\Delta V/cJ_1 = 0.02$; specific heat ratio, $\gamma = 1.2$; proportionality constant, $J_2/J_1 = 1.0$; harmonic amplitude ratio, $p_2/p_1 = 0.2$.

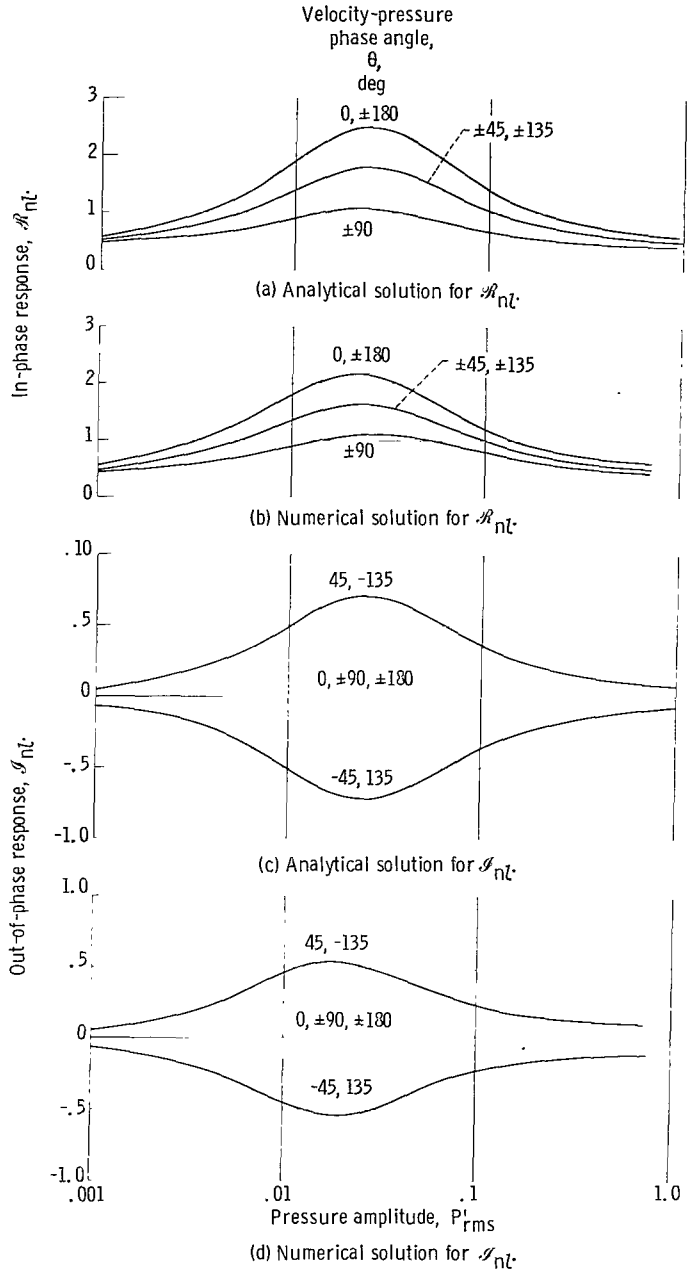

Figure 5. - Effect of velocity-pressure phase angle on response. Harmonic phase angle, $\varphi_2 = 0°$; relative axial Mach number, $\Delta\bar{V}/cJ_1 = 0.02$; specific heat ratio, $\gamma = 1.2$; proportionality constant, $J_2/J_1 = 1.0$; harmonic amplitude ratio, $p_2/p_1 = 0.2$.

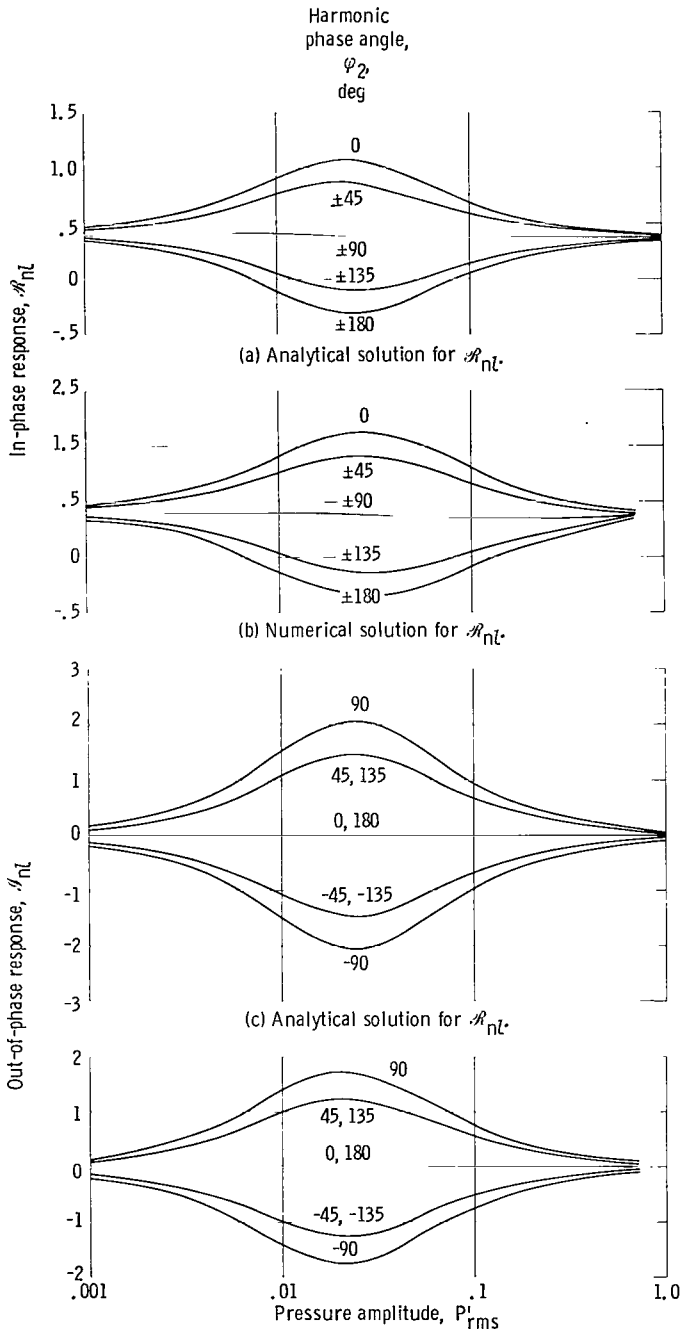

Figure 6. - Effect of harmonic phase angle on response for an out-of-phase velocity-pressure. Velocity-pressure phase angles, $\theta_1 = \theta_2 = 90°$; relative axial Mach number, $\Delta V/cJ_1 = 0.02$; specific heat ratio, $\gamma = 1.2$; proportionality constant, $J_2/J_1 = 1.0$; harmonic amplitude ratio, $p_2/p_1 = 0.2$.

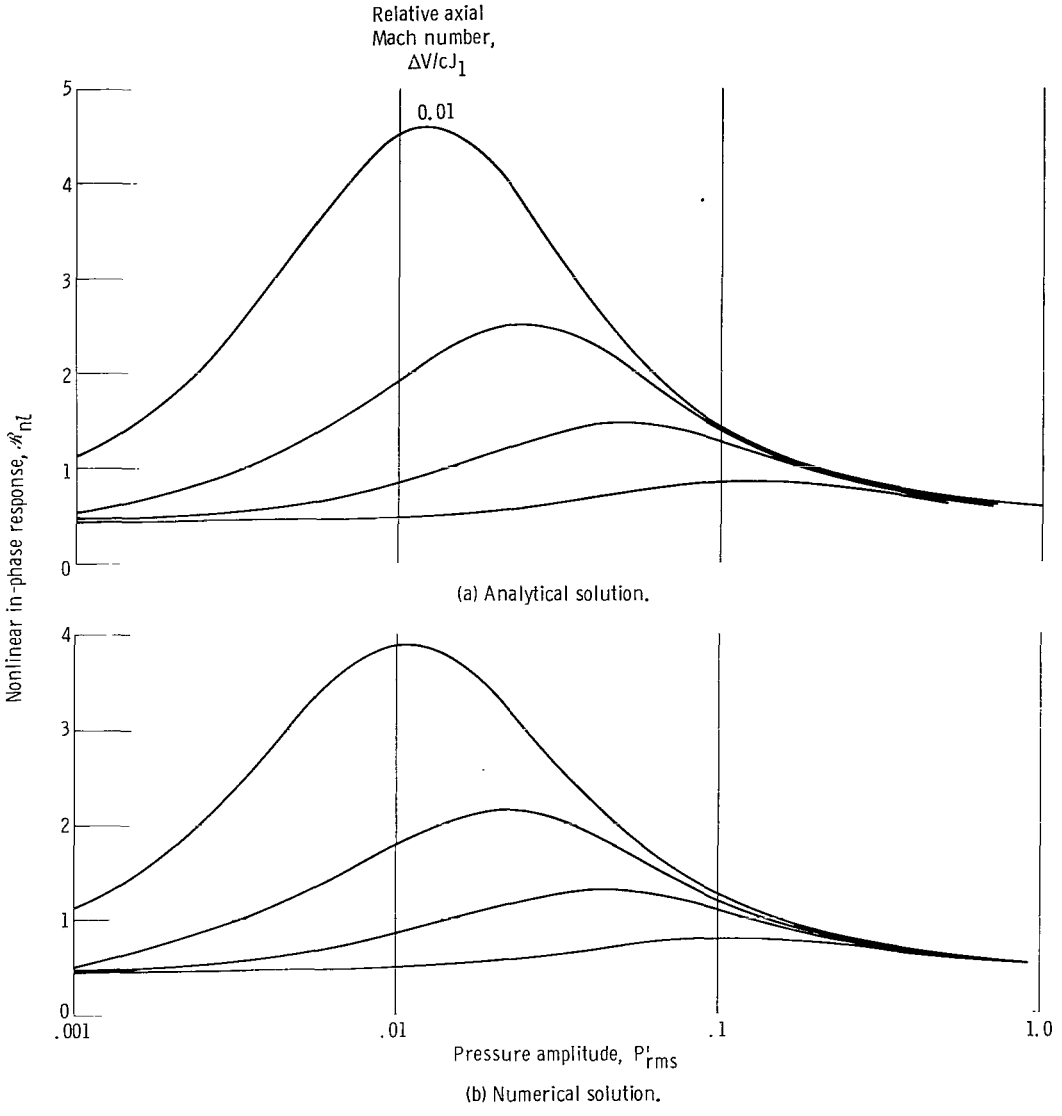

Figure 7. - Effect of relative axial velocity on response. Harmonic phase angle, $\varphi_2 = 0°$; velocity-pressure phase angles, $\theta_1 = \theta_2 = 0°$; specific heat ratio, $\gamma = 1.2$; proportionality constant, $J_2/J_1 = 1.0$; harmonic amplitude ratio, $p_2/p_1 = 0.2$.

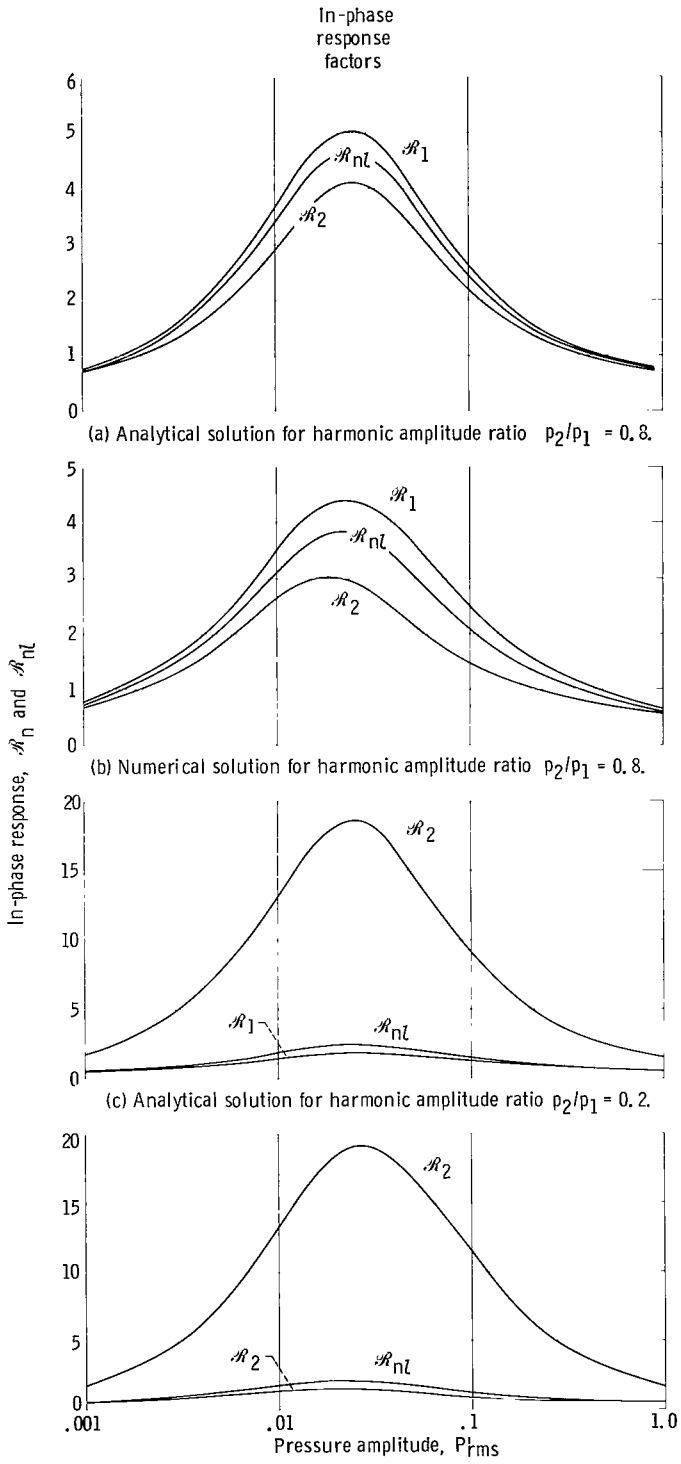

(a) Analytical solution for harmonic amplitude ratio $p_2/p_1 = 0.8$.

(b) Numerical solution for harmonic amplitude ratio $p_2/p_1 = 0.8$.

(c) Analytical solution for harmonic amplitude ratio $p_2/p_1 = 0.2$.

(d) Numerical solution for harmonic amplitude ratio $p_2/p_1 = 0.2$.

Figure 8. - Comparison of harmonic and nonlinear in-phase responses. Harmonic phase angle, $\varphi_2 = 0°$; velocity-pressure phase angles, $\theta_1 = \theta_2 = 0°$; relative axial Mach number, $\Delta\bar{V}/cJ_1 = 0.02$; specific heat ratio, $\gamma = 1.2$; proportionality constant, $J_2/J_1 = 1.0$.

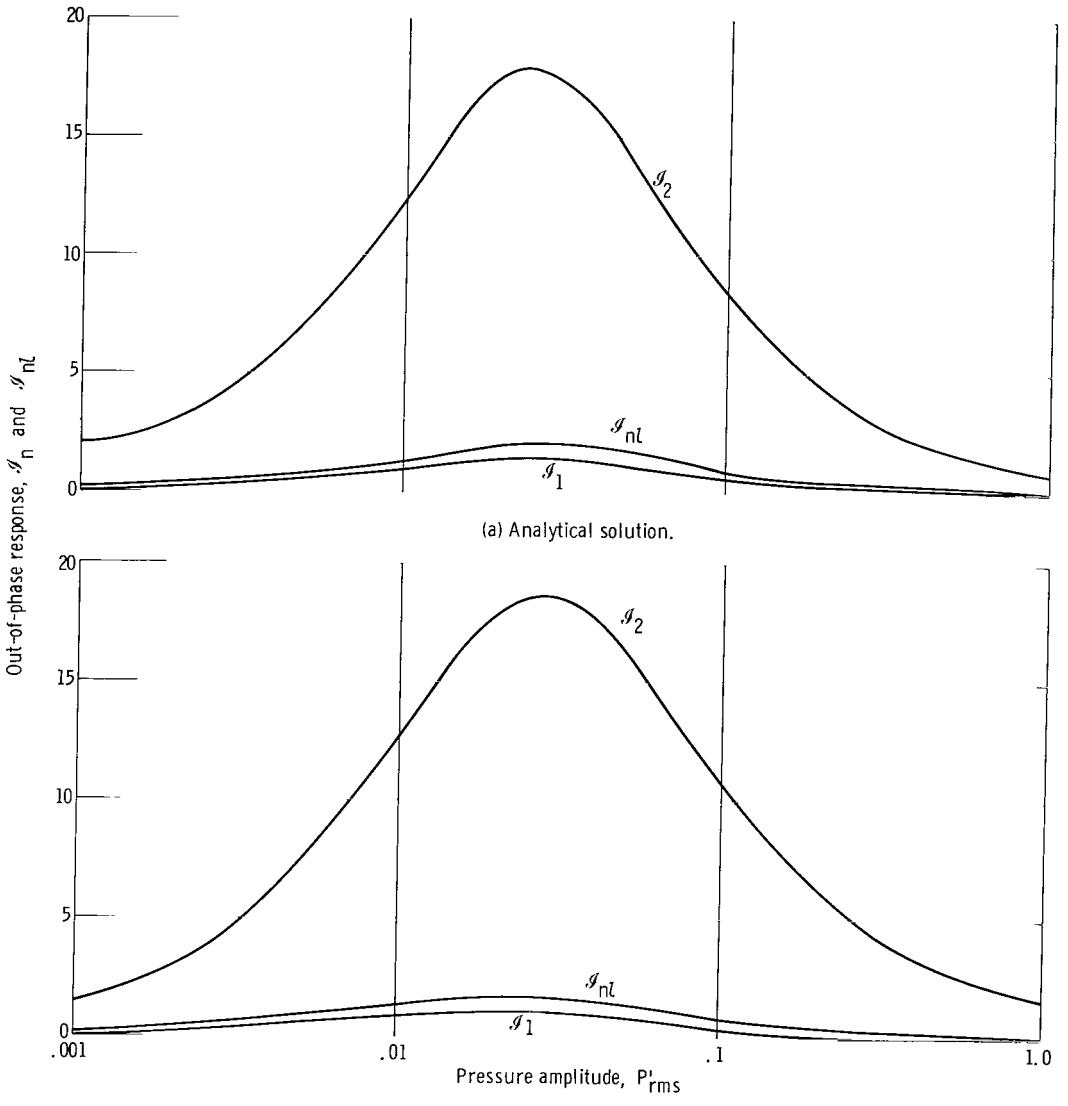

Figure 9. - Comparison of out-of-phase responses. Harmonic phase angle, $\varphi_2 = 90°$; velocity-pressure phase angles, $\theta_1 = \theta_2 = 90°$; relative axial Mach number, $\Delta V/cJ_1 = 0.02$; specific heat ratio, $\gamma = 1.2$; harmonic amplitude ratio, $p_2/p_1 = 0.2$.

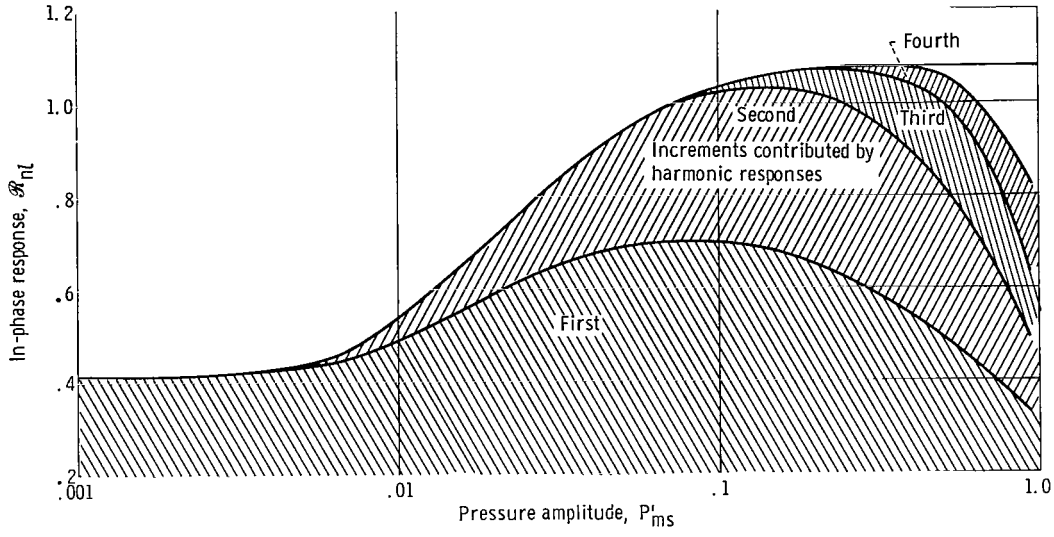

Figure 10. - Contribution of harmonic responses to nonlinear response for strong traveling waves. Numerical solution.

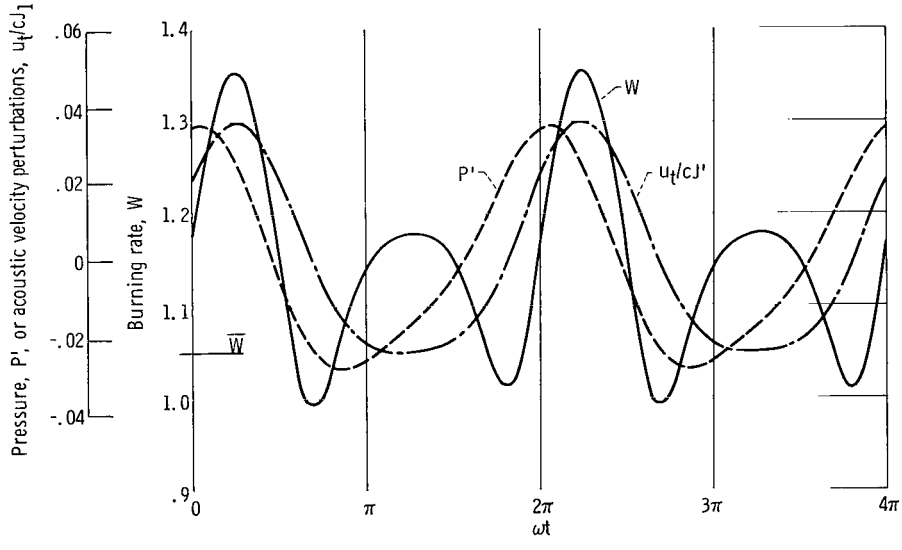

Figure 11. - Numerical evaluations of burning rate, pressure, and acoustic particle velocity perturbations. Harmonic phase angle, $\varphi_2 = 45°$; velocity-pressure phase angles, $\theta_1 = \theta_2 = 45°$; relative axial Mach number, $\Delta V/cJ_1 = 0.02$; specific heat ratio, $\gamma = 1.2$; proportionality constant, $J_2/J_1 = 1.0$; harmonic amplitude ratio, $p_2/p_1 = 0.2$; harmonic coefficient, $p_1 = 0.3$.

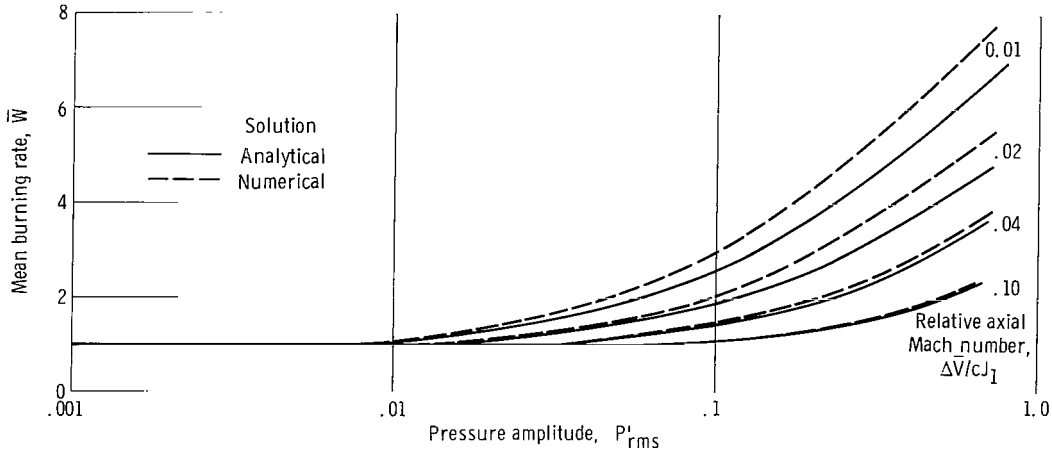

Figure 12. - Mean burning rates. Harmonic phase angle, $\varphi_2 = 0^c$; velocity-pressure phase angles; $\theta_1 = \theta_2 = 0°$; specific heat rates, $\gamma = 1.2$; proportionality constant, $J_2/J_1 = 1.0$; harmonic amplitude ratio, $p_2/p_1 = 0.2$.

NASA-Langley, 1971 —— 33 E-6049

"The aeronautical and space activities of the United States shall be conducted so as to contribute . . . to the expansion of human knowledge of phenomena in the atmosphere and space. The Administration shall provide for the widest practicable and appropriate dissemination of information concerning its activities and the results thereof."

—NATIONAL AERONAUTICS AND SPACE ACT OF 1958

NASA SCIENTIFIC AND TECHNICAL PUBLICATIONS

TECHNICAL REPORTS: Scientific and technical information considered important, complete, and a lasting contribution to existing knowledge.

TECHNICAL NOTES: Information less broad in scope but nevertheless of importance as a contribution to existing knowledge.

TECHNICAL MEMORANDUMS: Information receiving limited distribution because of preliminary data, security classification, or other reasons.

CONTRACTOR REPORTS: Scientific and technical information generated under a NASA contract or grant and considered an important contribution to existing knowledge.

TECHNICAL TRANSLATIONS: Information published in a foreign language considered to merit NASA distribution in English.

SPECIAL PUBLICATIONS: Information derived from or of value to NASA activities. Publications include conference proceedings, monographs, data compilations, handbooks, sourcebooks, and special bibliographies.

TECHNOLOGY UTILIZATION PUBLICATIONS: Information on technology used by NASA that may be of particular interest in commercial and other non-aerospace applications. Publications include Tech Briefs, Technology Utilization Reports and Technology Surveys.

Details on the availability of these publications may be obtained from:

SCIENTIFIC AND TECHNICAL INFORMATION OFFICE

NATIONAL AERONAUTICS AND SPACE ADMINISTRATION

Washington, D.C. 20546